



Half-metallic spin dynamics at a single LaMnO₃/SrMnO₃ interface studied with nonlinear magneto-optical Kerr effect

Naoki Ogawa,^{1,2,*} Takuya Satoh,³ Yasushi Ogimoto,^{1,2,†} and Kenjiro Miyano^{1,2}

¹Research Center for Advanced Science and Technology (RCAST), The University of Tokyo, Komaba, Meguro-ku, Tokyo 153-8904, Japan

²CREST, Japan Science and Technology Agency, 4-1-8 Honcho, Kawaguchi, Saitama 332-0012, Japan

³Institute of Industrial Science (IIS), The University of Tokyo, Komaba, Meguro-ku, Tokyo 153-8904, Japan

(Received 18 September 2009; published 10 December 2009)

Electronic and magnetic dynamics at a single interface of antiferromagnetic manganites, LaMnO₃/SrMnO₃, were studied with time-resolved second-harmonic generation and time-resolved nonlinear magneto-optical Kerr effect. The temporal evolution of the respective signals shows clear differences; an optical pump makes an instantaneous response of the electrons and, in contrast, induces slow demagnetization, which points to a possibility of two-dimensional half-metallic ferromagnetism for this heterointerface. Detailed analysis with various pump and probe polarizations reveals possible pathways of the optical charge-transfer excitation between Mn *d* orbitals, leading to a subsequent perturbation to the interface spin system.

DOI: [10.1103/PhysRevB.80.241104](https://doi.org/10.1103/PhysRevB.80.241104)

PACS number(s): 78.20.Ls, 42.65.Ky, 75.70.Cn

As invaluable magnetic materials for spintronic applications, half-metallic ferromagnets have been attracting much attention.¹ The perovskite manganites, such as La_{1-x}Sr_xMnO₃ (LSMO), have been shown to possess half-metallic nature with rich physics of charge and orbital degrees of freedom² and are now at the stage of designing new electronic phases by forming heterointerfaces with the help of state-of-the-art thin-film growth techniques. For example, at the interface of LaMnO₃ (LMO) and SrMnO₃ (SMO), both are insulating and antiferromagnetic in the bulk form (Fig. 1);^{3,4} the charge redistribution modifies the electronic and magnetic properties, leading to ferromagnetic and, in some cases, conducting states.⁵⁻¹² This interface electronic state is predicted to be a fully spin-polarized two-dimensional electron gas.^{13,14}

The dynamic aspects of the half-metallic ferromagnets are also of particular importance in terms of ultrafast manipulation of spin systems. In many optical pump-probe experiments, thermalization of quasiparticles was found to take place without a loss of magnetization.^{15,16} The subsequent slow demagnetization, usually detected through time-resolved (TR) magneto-optical Kerr effect (MOKE), manifests small electron-spin coupling and has been ascribed to the thermalization of the spin system with spin-lattice interaction.^{16,17} The time constants for this spin dynamics are determined by the spin-orbit interaction, i.e., magnetocrystalline anisotropy.¹⁸ A ferromagnetic state formed at the heterointerface can be viewed as ferrotoroidic with the induced interface dipole. In the TR second-harmonic generation (SHG) experiments on a bulk multiferroic GaFeO₃, time evolutions of the crystallographic polarization (*P*) and the toroidal moment (*T*) have been detected separately.¹⁹ However, the spin dynamics (magnetic moment *M*) was inferred indirectly from the combination with *P* ($T = P \times M$).

Up to now, most of the experimental works on the interface of LMO/SMO, including TR-MOKE,²⁰ have been performed on the superlattice structures, presumably to amplify the signal intensity. However, to obtain intrinsic information and for future applications, single interfaces should be examined. Nonlinear optical techniques, especially interface-

sensitive SHG, have been proven to meet with these demands.^{11,21}

In the present study, we investigated ultrafast electron and spin dynamics at the single heterointerface of LMO/SMO with TR-SHG and time-resolved nonlinear MOKE (TR-NMOKE). The interface electron and spin systems show distinct time evolution after optical excitation. The observed fast electron response and slow demagnetization are a common feature of half-metallic ferromagnets with a weak electron-spin coupling. This temporal demagnetization shows clear pump polarization dependence, whereas TR-SHG is least affected by the pump polarization, but varies depending on the probe polarization, i.e., elements of the nonlinear optical susceptibility tensor. We found that the orbital alignment and resultant transition dipoles are responsible for the anisotropy in the electronic excitation and relaxation pathways.

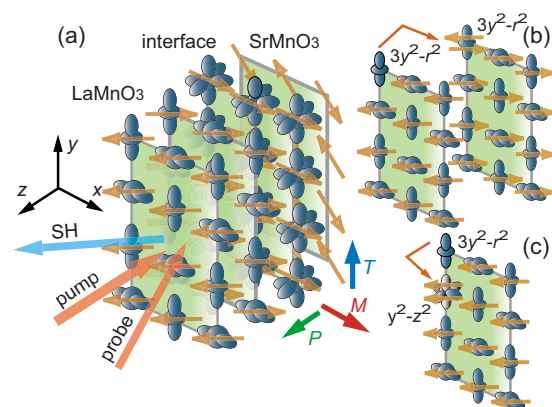


FIG. 1. (Color online) (a) Experimental coordinates and schematic illustration of the interface of LaMnO₃/SrMnO₃ double layer. LaMnO₃ (*d*⁴) and SrMnO₃ (*d*³) are anticipated to be A- and G-type antiferromagnetic insulators, respectively (Ref. 4). The alternating alignment of *d*_{3x²-y²} and *d*_{3y²-z²} orbitals in LaMnO₃ and an orbital-mixed ferromagnetic state at the heterointerface are expected. (b) and (c) Illustrations for the interlayer and intralayer optical transitions.

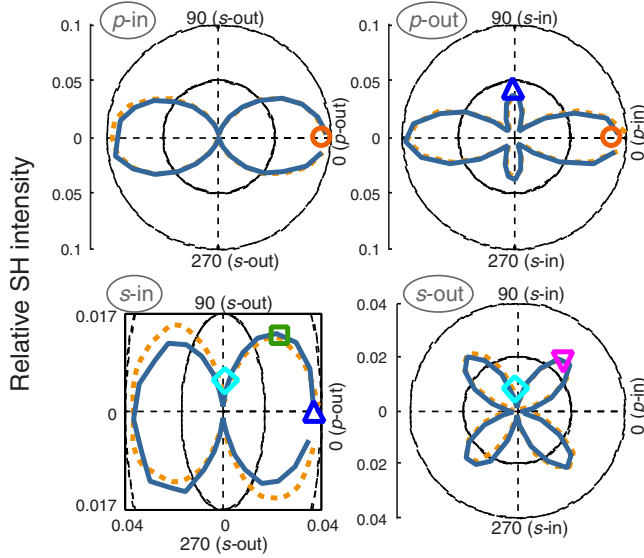


FIG. 2. (Color online) SH polarization diagrams for the $\text{LaMnO}_3/\text{SrMnO}_3$ heterointerface at 30 K. Solid (dotted) lines indicate the signals under the in-plane magnetic field $B = 0.1$ (-0.1) T. The nonlinear magneto-optical Kerr rotation can be seen in s -in geometry (magnified in the vertical axis for clarity). Open marks show the polarization configurations used for time-resolved measurements in Fig. 3.

A double layer, LMO on SMO, was prepared on a $(\text{LaAlO}_3)_{0.3}(\text{SrAl}_{0.5}\text{Ta}_{0.5}\text{O}_3)_{0.7}$ (LSAT) (001) substrate by pulsed laser deposition (for details, see Refs. 22 and 23). Both materials are approximately four unit cells (~ 1.6 nm) in thickness. SHG was measured in a UHV cryostat with 800 nm probe light (150 fs duration at 1 kHz repetition rate) with 90° reflection geometry. A pump light pulse from the same source was applied on the sample, with a 3° offset from the probe, after a delay line. A magnetic field was applied in plane (x direction in Fig. 1) with permanent magnets. TR-NMOKE was measured by analyzing the SH polarization with s -polarized incident light (Fig. 2). As reported previously, the sample undergoes a ferromagnetic transition at ~ 150 K,⁶ and the rotation angle of NMOKE closely follows the magnetization of the sample down to low temperatures.¹¹ In addition, confined electronic states were confirmed by measuring the directions of interface dipoles. The observed interface magnetism has been explained with the competition between antiferromagnetic superexchange of core spins and ferromagnetic double exchange mediated by the itinerant e_g electrons.¹³ We note that the SHG from the LSAT substrate is negligible. The pump and probe intensities are 3 and $1.25 \mu\text{J}$ on 150 and $100 \mu\text{m}$ ϕ spots, respectively, which were finely chosen to avoid a damage on the sample and to induce detectable SHG. The fluence seems to be relatively large. However, the overall temperature rise must be negligible judging from the near coincidence of the temperature dependence of the Kerr rotation angle with that of the sample magnetization under the similar experimental setup.¹¹

An example of SH polarization diagram at 30 K is shown in Fig. 2 under the external magnetic field of ± 0.1 T. The heterointerface of LMO/SMO shows $4mm$ symmetry, as expected, which has three independent elements ($\chi_{zx}^d = \chi_{zy}^d$,

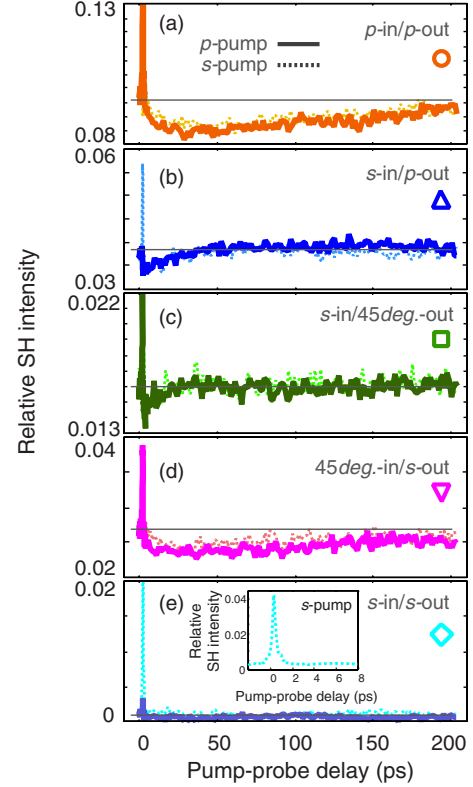


FIG. 3. (Color online) (a)–(e) Time-resolved SH signals for each polarization configuration at 30 K and under $B = -0.1$ T. Here 45° means mixed polarization. Solid (dotted) lines show the time evolution after p - (s -) polarized pump excitation. Thin horizontal lines indicate the SH intensity without a pump. Inset in (e) shows an instantaneous response around 0 ps for s -in and s -out configurations. Each signal contains the information of the following tensor elements: (a) p -in/ p -out ($\chi_{zx}^d, \chi_{zx}^d, \chi_{zz}^d$), (b) s -in/ p -out (χ_{zy}^d), (c) s -in/ 45° -out (χ_{zy}^d, χ_{yy}^m), (d) 45° -in/ s -out (χ_{zy}^d, χ_{yy}^m), and (e) s -in/ s -out (χ_{yy}^m).

$\chi_{zx}^d = \chi_{zy}^d$, and χ_{zz}^d) in nonlinear optical susceptibility tensor $\chi^{(2)}$ (lattice dipole origin: d). The charge redistribution at the interface from LMO to SMO is within one to two unit cells,^{14,24} and the lattice is polarized to partly screen the potential difference,^{13,24} as has been predicted for $\text{LaTiO}_3/\text{SrTiO}_3$.²⁵ With the presence of magnetic moment at the interface, five additional tensor elements appear.²⁶ The NMOKE can be induced by χ_{yyy}^m , which is proportional to the toroidal moment,¹⁹ as is clearly observed as a polarization rotation in the s -in configuration (Fig. 2), even from this single interface.¹¹

Figure 3 shows the time evolutions of the SH intensity after the pump excitation at 30 K. The corresponding polarization configurations are indicated in Fig. 2. It was found that there is almost no pump polarization dependence except for at time zero. However, the relaxation characteristics show clear variations with probe polarization. The SH intensity shows faster relaxation (20–50 ps) for the s -polarized probe [Figs. 3(b) and 3(c)], whereas Figs. 3(a) and 3(d) reveal slow (>200 ps) recovery with minima around 30–40 ps for p and mixed probe polarization. The reversal of the magnetic field (± 0.1 T) did not make qualitative differences (not shown).

Note that it was difficult to directly observe the dynamics of the toroidal moment [Fig. 3(e)] due to the small signal intensity for the *s*-in/*s*-out geometry.

First, we discuss the absence of the pump polarization dependence in TR-SHG. There are several pathways for the pump excitation in this heterostructure; optical transitions in LMO, across the interface, inside the interface, and in SMO. The latter two processes are not relevant because SMO has relatively small optical conductivity at the pump energy,²⁷ and the interface with the orbital-liquid state is presumably isotropic within the interfacial plane. From first-principles calculations,^{14,28,29} the optical charge-transfer (CT) transition would proceed between neighboring e_g orbitals for LMO and across the interface. Here, possible effects of *p*-*d* hybridization³⁰ are neglected for simplicity. According to the previous pump-probe spectroscopy on a LMO film,³¹ the absence of the pump polarization dependence can be explained with the coincident final state after the optical excitation; if we start with an occupied Mn $d_{3y^2-r^2}$ orbital in LMO [Figs. 1(b) and 1(c)], the spin-conserving CT transition is to the interplane $d_{3y^2-r^2}$ orbital (for *p* pump) and to the in-plane neighboring $d_{y^2-z^2}$ (for *s* pump), where originally the former is half occupied by the majority spin and the latter is empty, and both are 1–2 eV above the ground state.²⁹ The successive in-plane transfer is prohibited due to the small transfer integral. The energy of the both excited states is nearly degenerate with that of the available orbitals in the neighboring planes, thus forming a conduction band along the *c* axis irrespective of the initial pump polarization. Accordingly, the excited electrons are mobile in the *c* direction even with the orbital- and spin-ordered ground states, which affects the interface electronic state and leads to the large anisotropy in the subsequent SHG.

After the pump irradiation, the SH intensity temporally decreases due to the bleaching of the CT excitation, increase in the lattice temperature, and screening of lattice polarization by the excited quasiparticles³² (Fig. 3). The relaxation proceeds with the recovery of the orbital order, which will be in the time scale of 10 ps as reported for a LMO film.³¹ Thus, the time evolution for *s*-in probe geometry [Figs. 3(b) and 3(c)] can be ascribed to this orbital motion. The slow relaxation observed for the *p*-in probe can be explained by the inherent large anisotropy at the heterointerface and existence of the pump-induced conduction band along the *c* axis, which would help one to screen the interface with large lattice motion.¹³

Figure 4 shows the demagnetization dynamics at 30 and 150 K. This TR-NMOKE can be resolved only at lower temperatures (below $T_C \sim 150$ K) and shows a clear difference between *p*- and *s*-pump excitations, which is distinct from the case of the TR-SHG. For each pump polarization, the magnetic moment at the interface starts to decrease in a similar manner up to ~ 40 ps, has a minimum (~ 120 ps for *p* pump and ~ 75 ps for *s* pump), and shows a recovery of about 1000 ps. The time constant on the order of 100 ps for this demagnetization is common for half-metallic ferromagnets,¹⁶ and a similar value has been reported for a bulk LSMO.¹⁷

The decrease in the Kerr rotation angle, i.e., magnetic moment M at the interface, is caused by the thermalization of

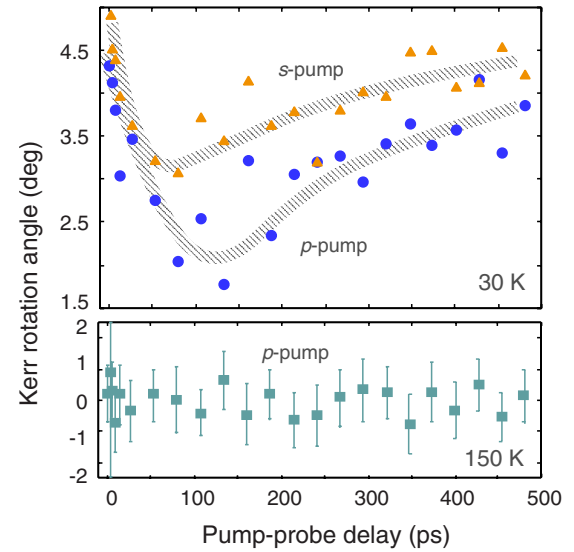


FIG. 4. (Color online) Time-resolved nonlinear magneto-optical Kerr rotation for the single LaMnO₃/SrMnO₃ interface at 30 and 150 K. The shaded lines are the guides to the eye. The error bars are omitted from the upper panel for clarity.

the spin system. The observed difference between *p*- and *s*-pump excitations in the TR-NMOKE signal indicates that, although the electronic final state is the same, the initial CT transition of the minority spin toward the interface in the *p*-pump configuration disturbs the spin system more efficiently. Since TR-SHG reflects the dynamics of electron and/or lattice system, the observed clear difference in the time evolution between TR-SHG and TR-NMOKE manifests weak couplings for electron-spin, and even for lattice-spin interaction. This weak electron-spin coupling indicates the half-metallic nature of this interface.¹⁶ We note that, in the current experiment, the TR-NMOKE can reveal nearly pure spin dynamics. Since the Kerr rotation angle is expressed as $\tan \theta \sim (T/P)$ for the *s*-in probe configuration, the modulation after the pump excitation is $\Delta(T/P) \sim \Delta M$ even when ΔT contains contributions both from ΔP and ΔM ; this is a different situation from detecting only the toroidally induced component.¹⁹

We also note that the spikelike components around 0 ps have been observed commonly in transient reflectivity and sometimes in TR-MOKE signals for many materials, which were discussed in connection with instantaneous electronic and magnetic excitations.¹⁶ Here, we observed similar features both in TR-SH and TR-NMOKE signals [Fig. 3(e) inset]. However, these involve other nonlinear effects due to the temporal overlap of pump and probe fields, which need further investigation. We observed almost the identical TR-SHG for a double layer with the reversed stacking order, i.e., SMO/LMO/LSAT. However, it was difficult to resolve TR-NMOKE for this sample due to its smaller Kerr rotation.¹¹

In summary, time-resolved nonlinear optical techniques were applied on the single interface of LMO/SMO. It was found that the electronic and magnetic signals show distinct

time evolution and pump-probe polarization dependences even at this single interface; the reflection TR-SHG shows no pump polarization dependence, whereas TR-NMOKE presents clear pump polarization dependence, which are explained by the selective optical excitation on the spin- and orbital-ordered ground states. The observed slow demagneti-

zation shows a weak electron-spin coupling, indicating a half-metallic nature of this heterointerface.

This work was partly supported by JSPS KAKENHI (Contract No. 21740243) and GCOE for Physical Sciences Frontier, MEXT, Japan.

*ogawa@myn.rcast.u-tokyo.ac.jp

[†]Also at Fuji Elec. Hold., Shinagawa, Tokyo 141-0032, Japan.

¹M. I. Katsnelson, V. Yu. Irkhin, L. Chioncel, A. I. Lichtenstein, and R. A. de Groot, *Rev. Mod. Phys.* **80**, 315 (2008).

²Y. Tokura and N. Nagaosa, *Science* **288**, 462 (2000).

³W. O. Wollan and W. C. Koehler, *Phys. Rev.* **100**, 545 (1955).

⁴Recently it was reported that both LaMnO₃ and SrMnO₃ epitaxial films are A-type antiferromagnetic on SrTiO₃(001) substrates, which, however, does not affect the discussion of the present data; S. J. May, P. J. Ryan, J. L. Robertson, J.-W. Kim, T. S. Santos, E. Karapetrova, J. L. Zarestky, X. Zhai, S. G. E. te Velthuis, J. N. Eckstein, S. D. Bader, and A. Bhattacharya, *Nature Mater.* **8**, 892 (2009).

⁵T. Koida, M. Lippmaa, T. Fukumura, K. Itaka, Y. Matsumoto, M. Kawasaki, and H. Koinuma, *Phys. Rev. B* **66**, 144418 (2002).

⁶N. Kida, H. Yamada, H. Sato, T. Arima, M. Kawasaki, H. Akoh, and Y. Tokura, *Phys. Rev. Lett.* **99**, 197404 (2007).

⁷Ş. Smadici, P. Abbamonte, A. Bhattacharya, X. Zhai, B. Jiang, A. Rusydi, J. N. Eckstein, S. D. Bader, and J.-M. Zuo, *Phys. Rev. Lett.* **99**, 196404 (2007).

⁸H. Yamada, M. Kawasaki, T. Lottermoser, T. Arima, and Y. Tokura, *Appl. Phys. Lett.* **89**, 052506 (2006).

⁹A. Bhattacharya, X. Zhai, M. Warusawithana, N. Eckstein, and S. D. Bader, *Appl. Phys. Lett.* **90**, 222503 (2007).

¹⁰C. Adamo, X. Ke, P. Schiffer, A. Soukiassian, M. Warusawithana, L. Maritato, and D. G. Schlom, *Appl. Phys. Lett.* **92**, 112508 (2008).

¹¹N. Ogawa, T. Satoh, Y. Ogimoto, and K. Miyano, *Phys. Rev. B* **78**, 212409 (2008).

¹²S. Dong, R. Yu, S. Yunoki, G. Alvarez, J.-M. Liu, and E. Dagotto, *Phys. Rev. B* **78**, 201102(R) (2008).

¹³B. R. K. Nanda and S. Satpathy, *Phys. Rev. Lett.* **101**, 127201 (2008).

¹⁴B. R. K. Nanda and S. Satpathy, *Phys. Rev. B* **79**, 054428 (2009).

¹⁵T. Kise, T. Ogasawara, M. Ashida, Y. Tomioka, Y. Tokura, and M. Kuwata-Gonokami, *Phys. Rev. Lett.* **85**, 1986 (2000).

¹⁶G. M. Müller, J. Walowski, M. Djordjevic, G.-X. Miao, A.

Gupta, A. V. Ramos, K. Gehrke, V. Moshnyaga, K. Samwer, J. Schmalhorst, A. Thomas, A. Hütten, G. Reiss, J. S. Moodera, and M. Münzenberg, *Nature Mater.* **8**, 56 (2009).

¹⁷T. Ogasawara, K. Ohgushi, Y. Tomioka, K. S. Takahashi, H. Okamoto, M. Kawasaki, and Y. Tokura, *Phys. Rev. Lett.* **94**, 087202 (2005).

¹⁸W. Hübner and K. H. Bennemann, *Phys. Rev. B* **53**, 3422 (1996).

¹⁹M. Matsubara, Y. Kaneko, J.-P. He, H. Okamoto, and Y. Tokura, *Phys. Rev. B* **79**, 140411(R) (2009).

²⁰H. B. Zhao, K. J. Smith, Y. Fan, G. Lüpke, A. Bhattacharya, S. D. Bader, M. Warusawithana, X. Zhai, and J. N. Eckstein, *Phys. Rev. Lett.* **100**, 117208 (2008).

²¹H. Yamada, Y. Ogawa, Y. Ishii, H. Sato, M. Kawasaki, H. Akoh, and Y. Tokura, *Science* **305**, 646 (2004).

²²T. Satoh, K. Miyano, Y. Ogimoto, H. Tamaru, and S. Ishihara, *Phys. Rev. B* **72**, 224403 (2005).

²³T. Satoh, T. Lottermoser, M. Fiebig, Y. Ogimoto, H. Tamaru, M. Izumi, and K. Miyano, *J. Appl. Phys.* **97**, 10A914 (2005).

²⁴H. Nakao, J. Nishimura, Y. Murakami, A. Ohtomo, T. Fukumura, M. Kawasaki, T. Koida, Y. Wakabayashi, and H. Sawa, *J. Phys. Soc. Jpn.* **78**, 024602 (2009).

²⁵S. Okamoto, A. J. Millis, and N. A. Spaldin, *Phys. Rev. Lett.* **97**, 056802 (2006).

²⁶R.-P. Pan, H. D. Wei, and Y. R. Shen, *Phys. Rev. B* **39**, 1229 (1989).

²⁷T. Satoh *et al.* (unpublished).

²⁸R. Søndénå, P. Ravindran, S. Stølen, T. Grande, and M. Hanfland, *Phys. Rev. B* **74**, 144102 (2006).

²⁹Y. Nohara, A. Yamasaki, S. Kobayashi, and T. Fujiwara, *Phys. Rev. B* **74**, 064417 (2006).

³⁰K. Tobe, T. Kimura, Y. Okimoto, and Y. Tokura, *Phys. Rev. B* **64**, 184421 (2001).

³¹H. Tamaru, K. Ishida, N. Ogawa, Y. Kubo, and K. Miyano, *Phys. Rev. B* **78**, 075119 (2008).

³²*Nonlinear Optics in Metals*, edited by K. H. Bennemann (Oxford University Press, New York, 1999).